

DESIGN, DEVELOPMENT AND PERFORMANCE CHARACTERISTICS OF
MULTI-RACK NATURAL CONVECTION SOLAR DRYER

BY

MOHAMMED A. HABIB

MECHANICAL POWER ENG. FACULTY OF ENG.
MENOUIYA UNIVERSITY, SHEBIN EL-KOM, EGYPT.

ABSTRACT:

The present work presents the construction and testing of a new design and performance characteristics of a multi-rack natural convection solar dryer for various types of crops. The dryer consists of a frustrum of pyramid shaped solar collector coupled directly with drying chamber in which drying trays are stacked one after the other at various levels in the dryer. The sloped plastic collector heats the air which passes by natural convection through the drying chamber where it removes water from the fresh crop. The cooled moist air then escapes to the open top of the drying chamber by the upward convection draught generated by the collector.

Two types of drying modes were used: (1) natural air circulation mode, and (2) open sun air-drying mode. The first one takes into account the treatment of each tray level individually and the dryer is treated as a whole unit. The results of experiments on grapes samples with different drying rate periods are presented. The paper also gives the mathematical equations that describe the performance characteristics of each tray level, the solar dryer and the open sun air-drying mode. It was found that the solar drying rates of grapes were faster and higher for trays nearer to the collector as compared with the open sun air-drying, while that in the middle levels of the drying chamber have shown poor drying characteristics. However, the tray level located at the topmost part of the chamber gave moderate drying rates.

1. INTRODUCTION:

Solar energy utilization for drying of various agricultural products like fruits, vegetables and crops has been practiced in different parts of the world. Most of these dried products are obtained by continuously exposing it to direct

**MANUSCRIPT RECEIVED FROM DR: HABIB M. A. AT:25/2/1996,
ACCEPTED AT:24/3/1996, PP 23 - 47
ENGINEERING RESEARCH BULLETIN, VOL, 19, NO. 2, 1996
MENOUIYA UNIVERSITY, FACULTY OF ENGINEERING,
SHEBINE EL-KOM, EGYPT. ISSN. 1110 - 1180**

open-sunshine without any technical aids [1]. The introduction of solar crop dryers seems to be an effective way to reduce crop losses and improve the quality of the dried product significantly compared to traditional drying methods [2]. There are basically two types of solar dryers; (1) a passive or natural system which operates only on solar energy alone without supplementary power source, and (2) an active or forced system which requires some supplementary power to circulate the air within the dryer unit [3, 4]. Solar dryers could be further classified as direct, indirect and mixed types [4, 5]. The direct type involves directly exposing the material to the sun while in the indirect type the material is dried by circulating hot air over it without directly exposing the material to sun rays. In mixed dryers, the product is dried by both direct radiation and hot flowing air. Solar drying systems also can be classified mainly on the basis of the mode of heat transfer employed, i.e. radiation or forced convection, free convection is present in both cases [6]. On the other hand, the dryer performance can be evaluated based on the method of treating the products inside the drying chamber, i.e.; either by treating the drying chamber as a whole unit with loading all trays [7] or by treating a single tray located at the center of the drying chamber [8, 9]. The merits of any solar dryer would depend upon the type and the quantity of product to be dried, the radiation level and the dryer treating method.

The efforts in studies on utilization of solar energy for drying different products were directed into two directions: improving the drying rate by understanding various parameters controlling it, and determining the relative advantages of the two modes of sun-drying and solar drying [10]. Wilson [11] and Szulmayer [12] had studied the effect of direct radiation and other parameters such as the influence of air temperature and humidity on the drying rate of sun-dried grapes. Their studies also were carried out on two different designs of solar dryers. In both cases, Wilson [11] had observed that the temperature of the untreated grapes exposed directly to solar radiation was 6-8 °C above the ambient temperature, while the corresponding temperature difference of treated grapes was only 4 °C. These studies have helped in establishing the superiority of sun-drying of grapes over solar drying. It was concluded that drying by hot air is equally good and the drying rate was almost equal for the two modes of drying. Simulation models and useful empirical relations are needed in the development of dryer designs and in the operation of drying systems. Zaman and Bala [8] presented thin layer drying rate equations for solar drying of rough rice for a mixed-mode dryer, a box-type dryer and an open floor drying system. Diamante and Munro [9] derived four mathematical models based on the diffusion type-equations to describe the solar drying of sweet potato slices. Several researches have developed design principals for natural air flow solar drying systems based on the chimney effect and using either psychrometry or thin layer drying equations for an exposed layer to develop the design [13-15]. Steinfeld and

Segal [16] have developed a simulation model for thin layer drying based on convection heat and mass transfer equations. Akyurt and Selcuk [17] reported the use of an exponential equation in fitting their solar drying data from a mixed mode dryer.

Some crops such as grapes, apricot and sweet potatoes need to be protected from direct solar radiation to avoid undesirable discoloration in the resulting product. These crops should therefore be dried in indirect solar dryers [9, 11, 18, 19]. Most of the solar drying studies have been achieved in indirect mode dryers with a single treatment mode. The main objective of the present work is: (1) to study the variations of drying air temperature at different locations inside the drying chamber using a new solar dryer, (2) to determine the drying characteristics of grapes taking into account both dryer treatment modes, and (3) to choose the best model that describes the grapes drying process under typical climatic Egyptian conditions. In addition, a comparative study of solar drying and open sun-drying modes was carried out. The empirical constants in Lewis, Fick, Page, Modified Page and Hale's models were found using the present experimental data and the results were compared with each other.

2. MATERIALS AND METHODS:

2.1 Solar dryer:

A passive plastic solar dryer was tested in the present experiments. Only readily available local materials were used in construction of the dryer. No electrical input was used which made it more applicable in the process of drying for different products. The designed, constructed and experimentally tested unit is shown in Fig. 1. The unit consisted of two main parts: a solar collector and a drying chamber. The solar collector was in the shape of a frustrum of a pyramid whose smallest area was connected directly with the base of the drying chamber. The bottom base of the solar collector dimension is 2.2x2.2 m. Galvanized iron sheets, black painted, were used to absorb the incident solar energy. A total of 42 iron sheets 2 mm thick, 5 cm wide and tilted at an angle of 30° from the horizontal were uniformly distributed, 2.5 cm apart, over the entire board. The construction of the absorbed surface using this method increases the surface area, air-flow turbulence and directs the incoming flow into a longer path. The total area of the plate was 9.24 m². The drying chamber was constructed of 5 mm thick aluminum sheets and has a square cross section with dimensions of 50x50 cm. A single transparent plastic cover was used for the framed collector and the drying chamber constructions.

Eight horizontal drying trays were arranged in one column of eight rows, one after the other. Each tray, Fig. 1, has a height of 4 cm and measures 5x5 cm. The drying trays were made

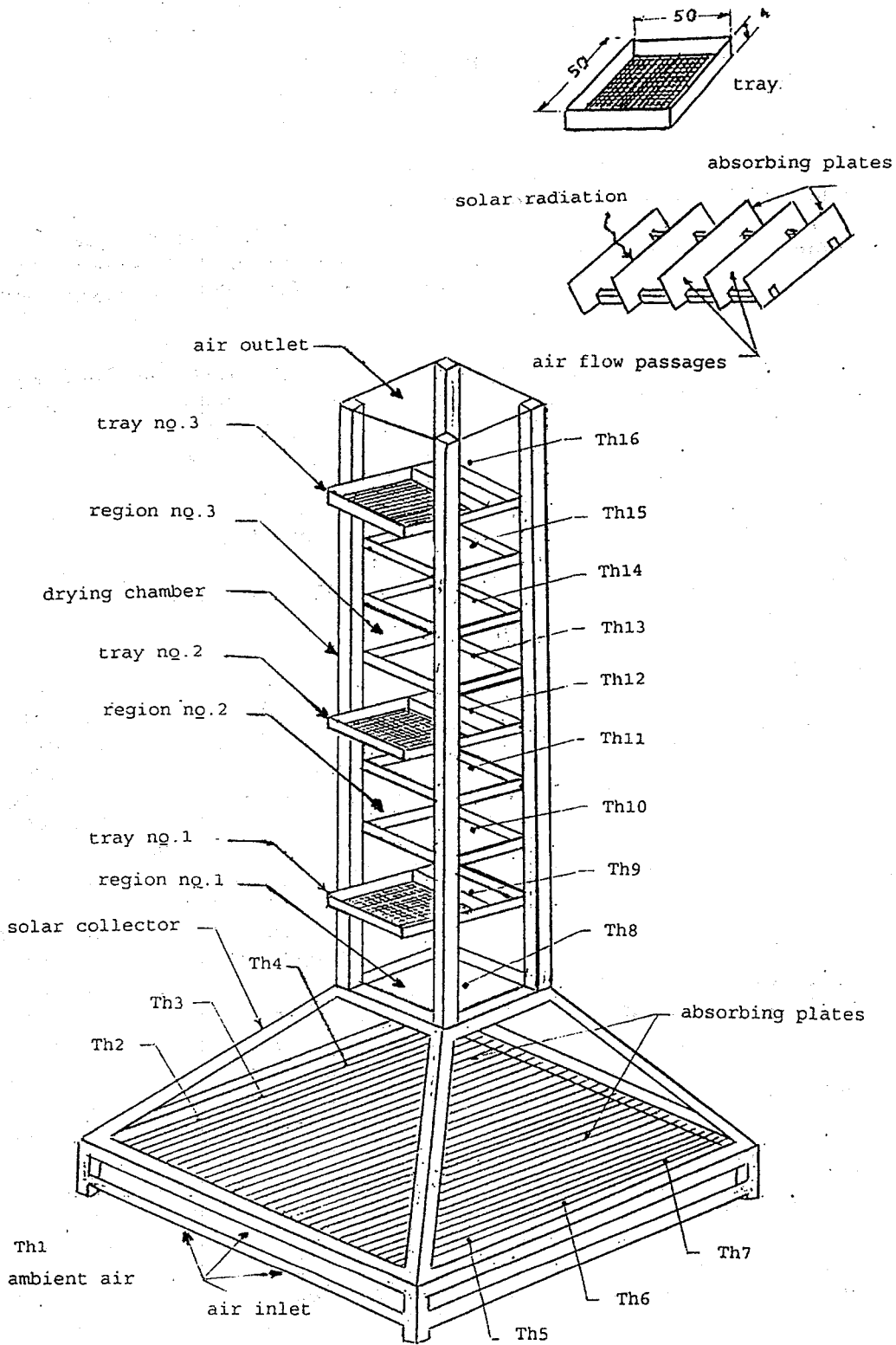


Fig. 1: Schematic diagram of the tested solar dryer.

Th1 to Th16 are thermocouples positions.

Dim. in cm.

of an aluminum frame all over the four sides and a wire mesh in the bottom to hold the samples. The trays were inserted and removed from their respective sides through small slits provided for this purpose. After the tray was put into its position, the slits were closed. The air enters through the absorbing surfaces in the base of the collector, heated initially by radiation from the surfaces lower parts, rises through the collector, enters the drying chamber and escapes from its open top by the upward convection draught. The advantages of this type of dryer over the conventional types are low cost, simplicity of construction, ease of handling and maintenance.

2.2 Solar drying experiments:

The solar drying experiments were carried out during the period of July 1995 at Shebin El-Kom, Egypt. Shebin El-Kom is at a latitude of 30.5° N. The range of climatic conditions during this period are: an ambient air temperature of $28-35^{\circ}$ C and 44-70 % relative humidity during the day. The insolation rate is about 320 w/m^2 per day. The grapes used in these experiments were obtained from a public market and were cleaned from dirt, green stems and destroyed pieces. The samples were spread on a drying tray which was then placed on the different levels of the drying chamber. A total of three trays were chosen to perform the drying process. One was loaded at the first level of the drying chamber near to the collector (tray number 1). The second tray was loaded at the fourth level in the middle of the drying chamber (tray number 2). The third was loaded at the eighth level in the top of the chamber (tray number 3). Another sample of grapes were put in open air and exposed directly to sun rays. The samples in each tray and that in the open air were about 6.5 mm thick. Each test run started at 9:00 A. M. and continued until 7:00 P. M. For each test, four samples of an initial weight of 500, 501, 661, 430 gm were placed on the first, second, third trays in the drying chamber and in the open air respectively. The average loading density is 2.28 kg/m^2 . The samples were distributed in the form of a thin layer to receive the same required amount of solar energy.

During each test the weights of trays were weighted periodically using an electronic balance of 0.001 gm sensitivity by removing them from the unit for approximately 20-30 seconds. The ambient dry bulb temperatures and temperatures inside the dryer were measured by copper - constantan thermocouples connected to digital thermometer with an accuracy of 0.1° C. The drying chamber temperatures were measured at 9 different positions and the thermocouples were suspended horizontally in the center of the chamber directly above each drying tray as shown in Fig 1. The ambient wet bulb temperatures were measured by a mercury in glass thermometer with an accuracy of $+ 0.5^{\circ}$ C. Collector inlet temperatures were measured at 6 different positions mounted at the entrance of the absorbing plates and the average value was considered.

Using the recorded values of initial weight W_o , weight of humid material at time (t) W_t , weight of dry material at the end of the test W_d , the values of initial moisture content M_o , moisture content M , drying rate dM/dt and moisture ratio MR could be determined. The moisture content at any drying time based on a percent dry basis was calculated using the following relationship [8]:

$$M = (W_t/W_o)(1-M_o)-1 \quad (1)$$

The variation in moisture content with time is given by:

$$\Delta M/\Delta t = -(M_{n+1} - M_n)/(t_{n+1} - t_n) \quad (2)$$

where $[t_{n+1} - t_n]$ is the time interval.

The corresponding drying rate was calculated as follows:

$$dM/dt = - \Delta M/A \Delta t \quad (3)$$

where A is the heat and mass transfer area.

2.3 Mathematical modeling of solar drying curves:

The solar drying curves were fitted with five different models applicable to higroscopic products [9, 15, 20] according to two different modes:

1. By treating the experimental data of each tray individually, then the drying characteristic and the empirical equation for a given tray can be obtained.
2. By treating the experimental data of all trays, then a general drying characteristic and an empirical equation for grapes using the dryer can be obtained. This will be expressed as a unit solar drying.

In addition, the sun-drying curves were fitted with the same models and a comparative study was presented. However, the moisture ratio MR was simplified to M/M_o instead of the term $(M-M_e)/(M_o-M_e)$ used by [21]. There are four reasons for this simplification:

1. Accurate M_e data are not available for grapes at different drying chamber temperature levels.
2. In solar drying the relative humidity of the drying air continuously fluctuated so that at least a mean value M_e could be calculated.
3. The results obtained by Hale [20] showed that the value of M_e has a relatively small effect on the values of the drying coefficients of the used exponential function.
4. Approximate calculations carried out by Diamante and Munro [9] indicated that M_e was less than 2 % at high

temperatures. Therefore, the error involved in the simplification was very small.

The different mathematical models derived in the present work are shown in Table 1. A computer program was used to carry out the regression analysis. The coefficient of determination r^2 was the primary criterion for selecting the best equation to describe the solar and sun-drying curves of grapes.

Table 1: Different mathematical models for fitting solar drying curves.

Model Number	Name of model	Mathematical model	Equation number
1	Lewis's model, LM Exponential eq.	$MR = a \exp(-bt)$ $\ln MR = \ln a - (bt)$	(4)
2	Fick's diffusion model, (FDM).	$MR = a \exp(-ct/w^2)$ $\ln MR = \ln a - (ct/w^2)$	(5)
3	Page's model, (PM).	$MR = \exp(-zt^n)$ $\ln[-\ln MR] = \ln z + n \ln t$	(6)
4	Modified Page's model, (MPM).	$MR = \exp(-k[t/w^2]^n)$ $\ln[-\ln MR] = \ln k + n \ln(t/w^2)$	(7)
5	Hale's model, (HM)	$MR = \exp(-b[-\log_e(1-MR)]^m t)$ $\log_e[-\log_e MR - \log_e t] = \log_e B + m \log_e[-\log_e(1-MR)]$	(8)

3. RESULTS AND DISCUSSION:

3.1 Drying chamber temperature variations:

Few investigators studied the variations of air temperature inside the drying chamber at different tray levels. In the case of no-load, Sandhu et al [7] pointed out the gradual increase of air temperature with the rise of tray level for inclined multi-rack natural convection dryer. For the case of loaded trays, drying chamber temperature variations are missed in the available literatures.

Figure 2 illustrates the variations of ambient air temperature (T_a), collector inlet and exit temperatures (T_{ci} and T_{co}) as well as temperatures of air leaving tray levels number 1, 2, and 3 (T_1 , T_2 and T_3) with drying time. In Fig. 3, the variations of air temperature at different locations x/L inside the dryer are presented. From these figures, it can be seen that all parameters; T_a , T_{ci} , T_{co} , T_1 , T_2 and T_3 increase with the drying time approaching a maximum value of 38-47 °C at about 14:00 O'Clock. They then start to decrease towards sunset

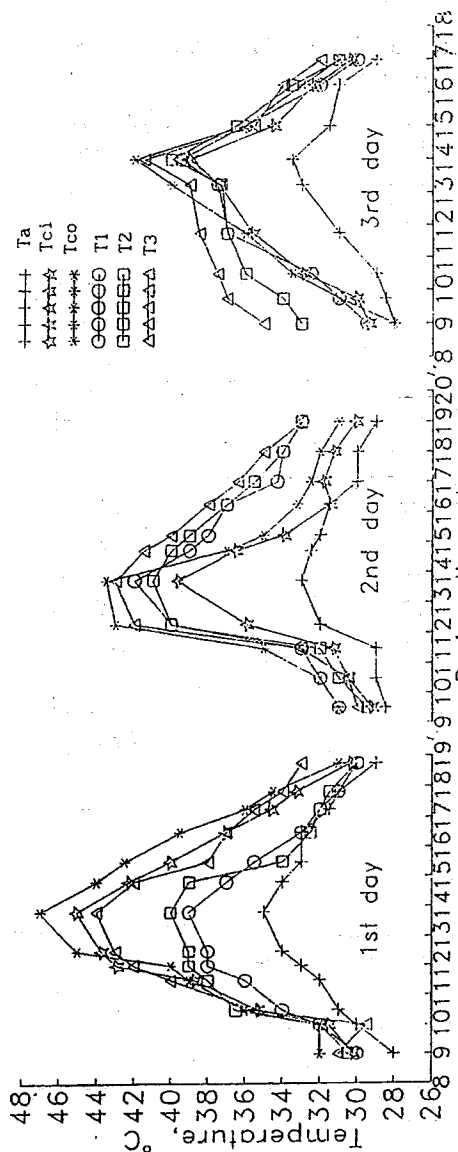


Fig. 2: Variations of ambient, collector and drying air temperatures with the drying time.

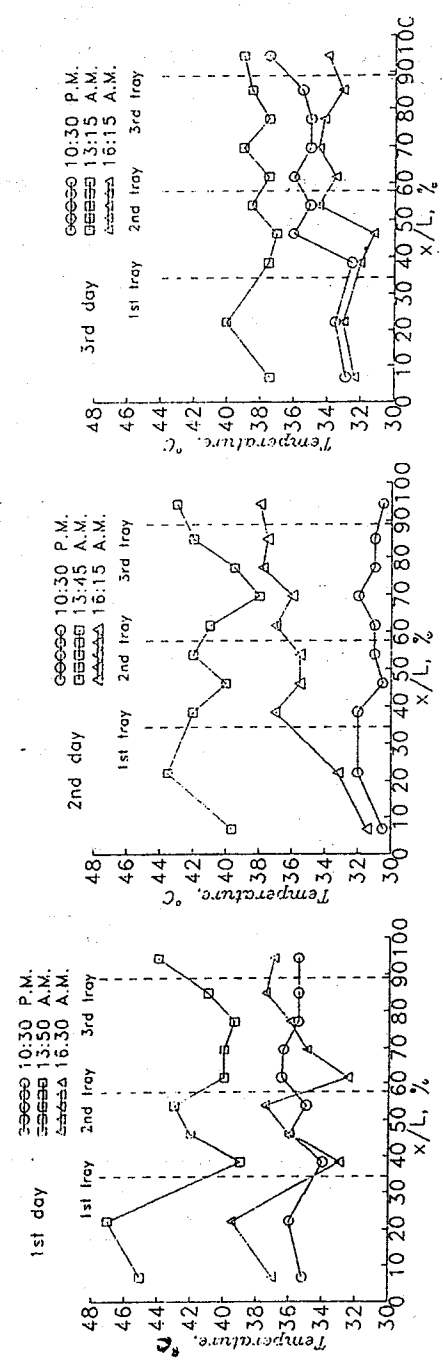


Fig. 3: Variations of drying air temperatures at different locations x/L inside the dryer.

time. Considerable improvement in collector inlet and outlet air temperatures with respect to the ambient air temperature can also be observed. The drop in air temperature between the inlet and outlet of the drying chamber was remarkable during the first day. On the second day, the drop in air temperature continued from 9:30 to 13:45 O'Clock A. M. where the percentage reduction in temperature ranged from 1.2 to 10.6 %. The drying air passing through the drying chamber absorbs the incident solar radiation and causes an increase of about 5.6 to 19.4 % in air temperature and resulted in a corresponding increase in drying rate of the third tray level. The results indicate that the percentage increase in dryer air temperature relative to ambient air temperature on the first, second and third days ranged from 2.7 to 30 %, 7.0 to 31.2 % and from 8.1 to 24.8 %, respectively. On the other hand, the percentage improvement in the collector air temperature relative to the ambient air temperature on the first, second and third days ranged from 5.8 to 31.5 %, 2.6 to 25.9 % and from 5.4 to 20.9 %, respectively.

For the first tray level, there is no change between the inlet and outlet drying air temperature during the first 1.5 hours over the drying period. After this period until the final stages of drying, the temperature of air leaving the first tray decreases compared with at the entrance temperature except for the period between 14:45 and 19:00 O'Clock P. M. on the second day. The increase of drying air temperature in the latter period could be attributed to (1): the moisture evaporation takes place at a slower rate from inside the product to the surface layer because of the completion of the removal of the product surface moisture and thus the surface has been dried, and (2): the additional drying potential of the air through the chamber cover. The decrease of grapes drying rate during this period was from 0.0155 to 0.0028 ($\text{kg}/\text{m}^2 \text{ hr}$), as seen in Fig. 4. The increase of drying air temperature was also observed for tray level number 2 at the same period, whereas the increase is earlier than that by about 3.25 hours for tray level number 3 and extended to the end of the drying process. The percentage reduction in drying chamber temperature between tray level number 1 ranged from 3.0 to 17.0 %. The percentage reduction (R_t) and improvement (I_t) in drying chamber temperature and the corresponding drying time (t) for each tray and in the region between trays are presented in Table 2.

The drying air leaving the first tray is influenced by the removal of moisture that has been extracted from the product. This air absorbs the incident solar radiation through the chamber cover (region 1) and causes an increase in its temperature. The air temperature in this region well depends on the amounts of both the absorbed energy and the evaporated moisture. The drying air temperature leaving the drying chamber is also affected by the removal of moisture from the product loaded in the three trays. The absorbed solar radiation and the fact that the surface of the third tray is directly exposed to

Table 2: The percentage reduction and improvement in drying chamber temperature.

Tray level and region		First day	Second day	Third day
Tray No. 1	Rt, % t, hr	0.0-17.0 09.00-18.45	0.0-7.0 09.30-13.45	0.0-6.3 09.00-17.00
	It, % t, hr	----- -----	5.4-10.5 14.45-19.00	----- -----
Region No. 1	Rt, % t, hr	0.0-6.3 09.00-10.00	0.0-4.1 09.30-19.00	----- -----
	It, % t, hr	2.8-13.6 10.30-18.45	----- -----	2.7-7.8 09.00-17.00
Tray No. 2	Rt, % t, hr	3.2-15.0 12.30-18.45	0.0-3.3 09.30-13.45	2.4-3.1 10.30-17.00
	It, % t, hr	4.3-6.7 10.00-11.30	2.6-4.2 14.45-19.00	2.9-2.1 09.0-9.45
Region No. 2	Rt, % t, hr	2.7-6.3 09.00-10.30	0.0-2.6 10.30-15.15	1.3-6.3 14.00-17.00
	It, % t, hr	1.5-15.4 11.30-18.45	0.0-2.0 16.15:18:00	1.4-3.2 09.0-13.25
Tray No. 3	Rt, % t, hr	0.0-1.7 09.00-12.00 15.30-18.45	0.0-1.6 09.30-10.30 -----	----- -----
	It, % t, hr	4.9-7.3 12.30-14.50	0.6-6.5 11.30-19.00	1.3-5.7 09.00-17.00
Drying chamber	Rt, % t, hr	1.2-10.6 09.00-17.50	1.2-5.7 09.30-13.45	1.2-2.5 13.15-15.00
	It, % t, hr	----- -----	6.5-14.5 14.45-19.00	5.6-19.4 09.00-11.45

the sun rays lead to an increase in the air temperature and consequently the drying rate. It was observed that the variations of air temperature before and after the second tray level as well as for region 2 was very small compared with that of the first tray, particularly on the second and third days. The experimental results show that the increase and/or drop in air temperature did not exceed 2.0 °C. The drying rate for the second tray level is expected to be the lowest.

3.2 Solar drying and drying rate curves:

Two forms of drying characteristics curves are plotted. The first form includes the solar drying curve which indicates the relationship between the moisture content and the drying time. The second form includes the drying rate curve which gives the drying rate versus the moisture content. These curves are characterized by three main periods. These are: warming-up period, constant drying rate period and the falling rate period. The warming-up period appears at the beginning of the drying process. The constant drying rate terminates at the critical moisture content and followed by the falling rate period. Different solids and different conditions of drying give different shapes of these periods.

Figure 4 presents the solar drying curve for grapes at the first, second and third tray levels as well as the solar and open sun-drying modes. Clear differences among the drying process of the three tray levels and also between the drying of grapes using solar and open sun-drying modes can be observed. For the first tray level, the moisture content reached 36 % at the end of the first day. It reduced to 8 % only at the end of the second day. However, at the end of the three days the samples were completely dried. The samples loaded in the first tray level had the highest drying rate compared with the other two trays and the two different modes of drying. For the second tray level, the results indicate that the moisture content reached 81.2 %, reduced to 40 % and then to 2 % at the end of first, second and third days, respectively. The drying process of grapes in the second tray was found to have the lowest drying rate. Figure 4 also shows that the drying process of grapes loaded in the third tray was faster on the first day than that of the second tray, while it gives lower drying rates than the first tray on the second and third days. In other words, the drying rate for the third tray was always lower than that of the first one for all drying times except for the first day. Comparing the other two drying modes, Fig. 4 indicates that the unit solar drying rate is relatively higher than that for open sun-drying mode at all drying periods except from 12:30 to 15:30 O'clock on the first day.

On the other hand, for drying grapes the maximum moisture content of 20% required for safe storage level can be achieved after 26 hours when the samples were loaded in the first tray. However, the drying time extended to 49.8 hours for that loaded in the second tray, while it took only 29 hours for the third tray level. If the samples were dried using solar drying mode, 31.5 hours are required to achieve the same safe storage value, whereas it is necessary to spread the samples 32.5 hours using sun-drying mode. The reduction in drying time between solar and sun-drying modes was 3.1 %. The drying time required to dry the samples in the second and third trays as well as the solar and sun-drying modes usually exceeds that required for the first tray.

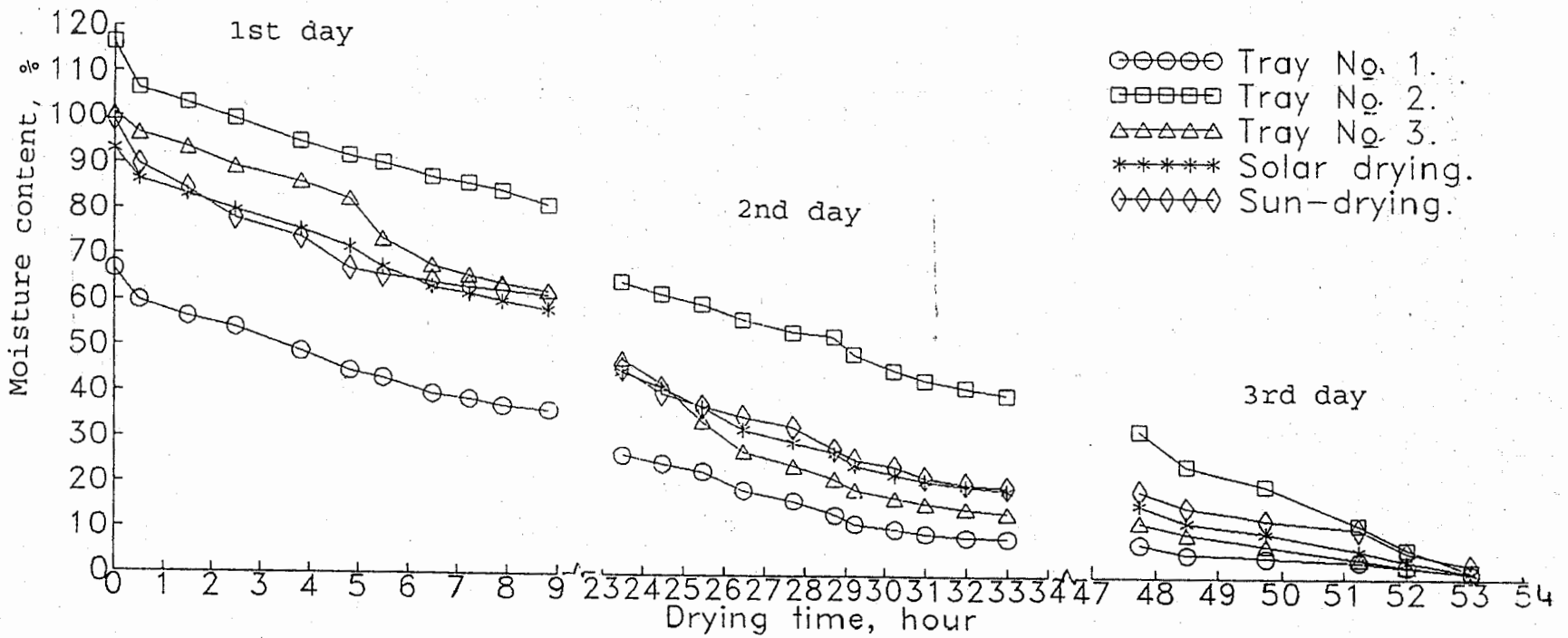


Fig. 4: Moisture content as a function of drying time.

To make additional comparisons between the drying process for different cases, the percentage reduction in moisture content has been introduced and the calculated results are given in Table 3. These values represent the overall percentage reduction in moisture content from the starting of drying to the final moisture content at the end of each drying day. Referring to Table 3, the percentage reduction in moisture content on the first and second days were 30.2 % and 38.1 %, respectively for the second tray compared with 45.9 % and 69% for the first tray level. At the end of the third day a faster and more complete drying was achieved using the first tray than that using the second one. The final moisture content of the second tray was about two times that of the first tray, so the reduction in moisture content seems to be higher. Qualitatively similar features can be found in Table 3 for the other drying modes.

Table 3: The percentage reduction in the moisture content under different drying cases.

Drying mode	Reduction in moisture content, %		
	First day	Second day	Third day
Tray No. 1	45.9	69.0	84.6
Tray No. 2	30.2	38.1	94.8
Tray No. 3	38.2	71.1	89.5
U.Solar drying	37.5	57.8	91.7
Sun-drying	38.1	56.9	85.1

The higher drying rate for the first tray level was due to the additional natural convection effect, caused by hot air flow through the products besides the incident rays through the chamber cover. For the second tray level, the air flow was always exposed to the moisture removed from the samples in the first tray causing its low drying rate. In the third tray, the drying process was affected by the direct incident rays on the upper surface of the sample besides the drying air coming from the collector. The incident rays have a strong effect during the first day, while the drying air has a strong effect during the second and third days. The absorption of solar radiation in the collector which exceeds that occurred by exposing the samples directly to sun radiation leads to the relative improvement in the drying rate for the solar drying mode. The short period of clear weather from 2.5 to 5.5 hours on the first day caused a rapid increase of about 3 °C in drying air temperature and resulted in a corresponding increase in drying rate.

In Figure 5, the drying rate is given for all cases as a function of moisture content. The drying process of grapes is characterized by the general following features:

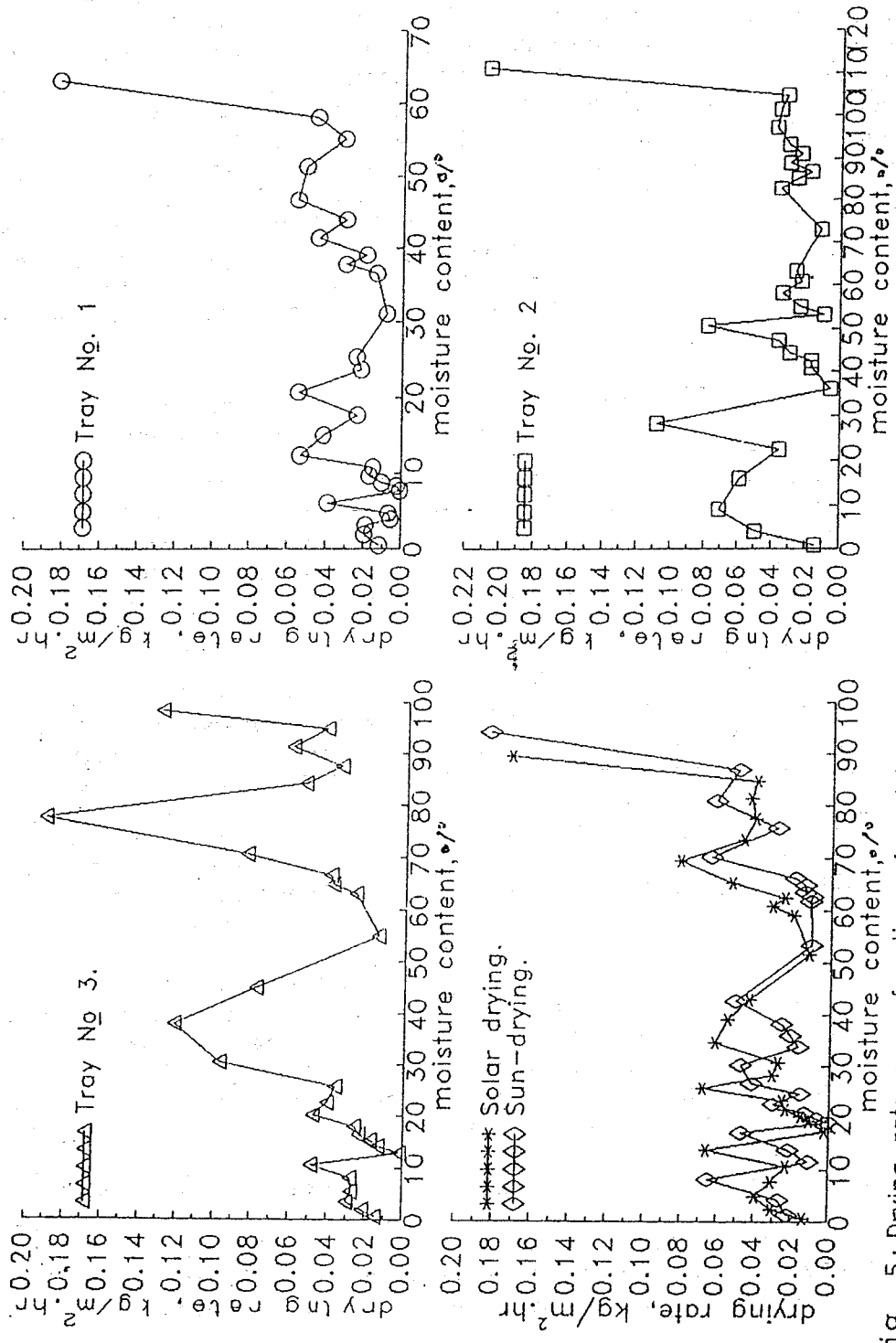


Fig. 5: Drying rate as a function of moisture content for different modes of drying.

- 1- A warming-up period which depends upon the tray level and the mode of drying. This period is characterized by a decrease in the drying rate with a corresponding decrease in the moisture content followed by an increase in the drying rate with a corresponding decrease in the moisture content. For the first tray level, the warming-up period took 1.75 hours and the moisture content decreased from 63.2 to 55.1 % which corresponded to moisture ratios of 0.949 and 0.828 and drying rates of 0.183 and 0.032 ($\text{Kg/m}^2 \cdot \text{hour}$), respectively. In the second stage, the period took 2.33 hours and the moisture content decreased from 55.1 to 46.9 % which corresponded to moisture ratios of 0.828 and 0.701 and drying rates of 0.032 and 0.056 ($\text{Kg/m}^2 \cdot \text{hour}$). This decrease in drying rate in the first stage is due to the lower liquid-surface temperature compared to that of the initial state which causes the curve to fall as shown in Fig. 5. In the second stage, the evaporation rate increases, while the samples surface temperature gradually rises.
- 2- No constant rate period was observed during the drying process of grapes for the three tray levels and the two modes of drying.
3. Five and/or six approximately linear falling rate periods were observed with transition periods between them and they depend upon the tray level and the drying mode. The transition periods represent the maximum drying rate and correspond to the drying chamber temperature and the maximum drying air temperature during the warmest period of the day. These dryer and air temperatures were much lower than the values reported by Zaman and Bala [8] for a mixed mode type dryer. All samples are clearly entering its falling rate period at a drying time period that ranged from 3.83 to 5.5 hours from the start. So, the drying rate falls. The first tray level exhibited five approximately linear falling rate continuing periods of 11.84, 1.13, 11.38, 2.37 and 2.0 hours with four transition periods between them. The corresponding maximum drying rates were 0.055, 0.053, 0.039, 0.019 ($\text{Kg/m}^2 \cdot \text{hours}$), respectively. The decrease in moisture content, moisture ratio and the corresponding drying rates during these periods are given in Table 4. A comparison between drying characteristics of different tray levels and the two modes of drying are also summarized in Table 4. All cases, except for tray level number 2, showed a significant decrease in the drying rate as the moisture content decreased in the first falling rate period that corresponds to a long drying period (11.0 to 11.84 hours). This period extended from 14:50 to 19:00 O'clock at the end of the first day. Also, the two last falling rate periods are characterized by a short drying times ranging between 1.0 to 2.37 hours.

For agriculture products there is usually no constant rate period [15]. The data of Diamante and Munro [21] exhibited no constant rate period and two linear falling rate periods with a

Table 4: Drying periods characteristics (D. CH.) for grapes using three tray levels and the two different modes of drying.

D. CH.	Tray No. 1	Tray No. 2	Tray No. 3	Unit Solar Drying	Sun-Drying
Mw1, % t, hr. dM/dt MR	63.2-55.1 1.75 0.183-0.032 0.949-0.828	111.3-104.7 0.75 0.208-0.032 0.957-0.899	98.6-87.7 2.92 0.130-0.036 0.980-0.870	89.7-84.7 0.75 0.173-0.041 0.964-0.910	94.4-75.8 2.92 0.184-0.029 0.952-0.765
Mw2, % t, hr. dM/dt MR	55.1-46.7 2.33 0.032-0.056 0.828-0.701	104.7-97.2 2.17 0.032-0.038 0.899-0.835	87.7-77.9 2.00 0.036-0.192 0.870-0.774	84.7-69.6 4.17 0.041-0.082 0.910-0.748	75.8-70.4 1.16 0.029-0.065 0.765-0.710
Mf1, % t, hr. dM/dt MR	46.7-31.2 11.84 0.052-0.009 0.701-0.468	97.2-86.7 3.71 0.038-0.017 0.835-0.745	77.9-54.9 11.0 0.192-0.015 0.774-0.545	69.6-51.5 11.0 0.082-0.012 0.748-0.553	70.4-53.3 11.84 0.065-0.011 0.710-0.538
Mf2, % t, hr. dM/dt MR	20.8-17.6 1.13 0.055-0.024 0.312-0.264	82.8-72.9 7.8 0.036-0.012 0.712-0.626	38.1-25.7 2.13 0.122-0.036 0.378-0.256	34.6-30.8 1.13 0.062-0.028 0.371-0.331	42.6-33.9 3.13 0.051-0.017 0.430-0.342
Mf3, % t, hr. dM/dt MR	12.3-7.7 11.38 0.053-9x10 ⁻⁴ 0.185-0.115	58.1-53.2 2.25 0.034-0.009 0.500-0.457	20.2-12.9 11.38 0.048-0.002 0.200-0.128	25.7-17.4 11.38 0.068-0.003 0.276-0.186	30.3-24.8 1.5 0.048-0.016 0.306-0.250
Mf4, % t, hr. dM/dt MR	6.1-3.97 2.37 0.039-0.006 0.091-0.06	50.8-36.2 11.38 0.078-0.005 0.437-0.311	10.7-5.7 2.37 0.049-0.027 0.107-0.056	13.9-10.8 1.0 0.067-0.023 0.149-0.116	22.8-19.2 9.75 0.031-0.0004 0.230-0.194
Mf5, % t, hr. dM/dt MR	3.1-0.55 2.0 0.019-0.012 0.050-0.009	28.4-22.4 1.0 0.108-0.035 0.244-0.192	3.5-0.63 2.0 0.030-0.015 0.035-0.006	4.90-0.66 2.0 0.039-0.014 0.053-0.007	17.1-11.6 2.37 0.047-0.011 0.173-0.117
Mf6, % t, hr. dM/dt MR	----- ----- ----- -----	9.1-0.85 2.0 0.071-0.014 0.078-0.008	----- ----- ----- -----	----- ----- ----- -----	8.2-1.42 2.0 0.065-0.022 0.083-0.015

Where Mw1 and Mw2 are the moisture contents at the first and the second warming-up periods, respectively. Mf1, Mf2,...etc are the moisture contents at the first, the second,...etc falling rate periods, respectively.

transition between them for forced convection drying of different variety of sweet potatoes. This contrasts with the drying rate curves for natural drying of sweet potato slices reported by the same authors [9], in which quite long constant rate period and one approximately linear falling rate period were exhibited. In the falling rate period the material surface is no longer saturated with water and the drying rate is controlled by diffusion of moisture from the interior of the solid to the surface. The rise of drying air temperature can be observed during this period.

3.3 Mathematical modelling of drying rates:

Each of the five drying curves were fitted to the five equations shown in Table 1. The computational results of the determination coefficient r^2 are presented in Table 5. Figures 6 through 10 show the experimental and fitted drying rate curves for all cases under consideration. The derived equations are also given in Figs. 6 through 10 at the upper right hand side of the graphs. All the used equations gave consistently high determination coefficient r^2 in the range of 0.9735 to 0.9138 except for Hale's model in which r^2 ranged from 0.5824 to 0.6985. This indicates that all the equations could satisfactorily describe the solar and sun-drying rates of grapes except for Hale's model that gave the worst fitting. The lowest r^2 values of 0.9138 and 0.9139 were for the exponential and diffusion equations, respectively, that used to fit the experimental data of tray level number 2. However, both Page and modified Page equations gave better results; $r^2=0.9202$. The tray level number 2 was installed in the middle part of the drying chamber which was exposed to the moisture evaporation coming from the first tray level. This leads to a continuous decrease in drying air temperature. The drying rate was correspondingly very low and the equation underpredicted the drying rate at the last 3.3 hours on the first day and at the first 7.5 hours on the second day, giving a relative rise to the value of r^2 . In the initial stages of drying, these two models (Page and modified Page equations) satisfactorily fitted the experimental data for tray level number 1 on the first day and up to moisture ratio of 0.775 (90.2 % moisture content) for tray level number 2. They were more accurate than the exponential and diffusion equations for all drying times. The exponential and Fick's diffusion equations resulted in almost the same values of r^2 for all cases, since very similar parameters were used in the models except for the presence of w^2 in Fick's equation. It is noticed that Fick's model is essentially the same as Lewis's model because (c/w^2) equals (b) in Lewis's model. Very close results could also be observed for Page and modified Page models.

Table 5: The computational results of the determination coefficient r^2 for different cases.

Model No.	Model Name	Tray No. 1	Tray No. 2	Tray No. 3	U.Solar Drying	Sun-Drying
1	Lewis's model	0.9687	0.9139	0.9675	0.9638	0.9572
2	Fick's model	0.9676	0.9138	0.9677	0.9621	0.9652
3	Page's model	0.9664	0.9202	0.9734	0.9674	0.9631
4	Modified Page's model	0.9702	0.9202	0.9735	0.9676	0.9632
5	Hale's model	0.6248	0.6074	0.6985	0.6634	0.5825

In most cases, the Page and modified Page equations gave values of r^2 (0.9202-0.9734) higher than those obtained for the exponential and Fick's equations (0.9138-0.9687). Fick's equation gave an r^2 value of 0.9652 for sun-drying mode which is higher than those of the modified Page and exponential equations and hence it could be adopted for modelling purposes. The results indicate that the modified Page equation was closer to the measured values only at the first stage of drying up to 62 % moisture content for tray level number 3, with the solar drying mode in all the drying times in the first day and for sun-drying up to 63 % moisture content. The modified Page equation was chosen over the exponential equation for curve fitting because it considers the thickness of the sample in calculations.

The poor fit of all cases using Hale's model clearly arises from the fact that the fitted equation grossly underpredicts the drying rate during the first 5.75 hours on the second day, during the first 0.75-2.0 hours on the third day and grossly overpredicts the drying rate in the later stages of the drying process. For the solar drying mode, Hale's model underpredicts the drying rate during the second day. The results show that the Hale's equation could satisfactorily describe the solar drying curves of grapes up to moisture contents of 36 % and 73.5 % for tray levels number 1 and 3, respectively.

The accuracy of the calculated values of moisture ratio depends largely on the model used in the calculations, the tray level and the mode of drying. The modified Page equation is better than the exponential equation for predicting the drying rate of grapes using both modes of drying, solar and open sun-drying. In most cases, the drying rate and the moisture ratio are very low, particularly, in the later stages of drying at the end of each day because of the reduction in drying air temperatures. This leads to an overprediction of the drying characteristics using the mathematical models and consequently

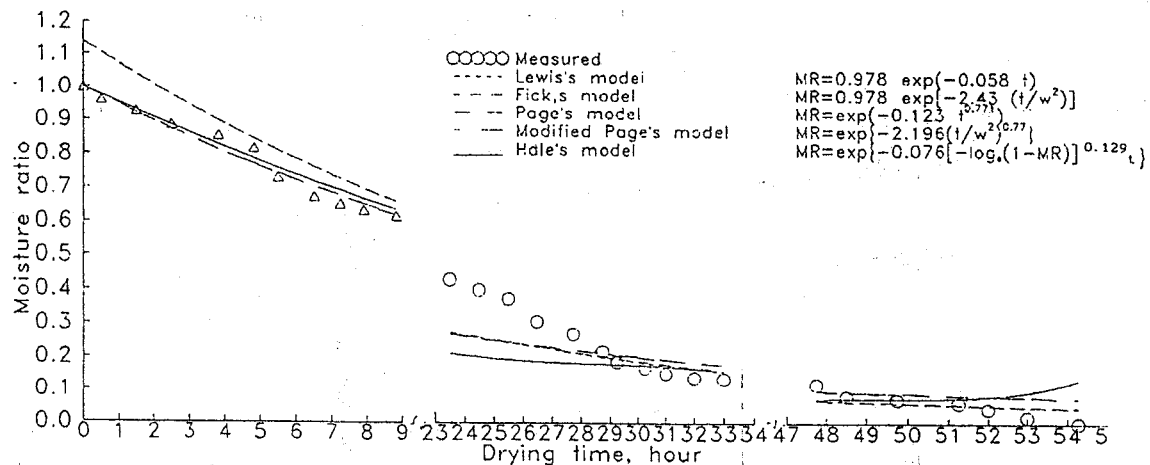


Fig. 6: The predicted moisture ratios during solar drying of grapes for tray level number 1.

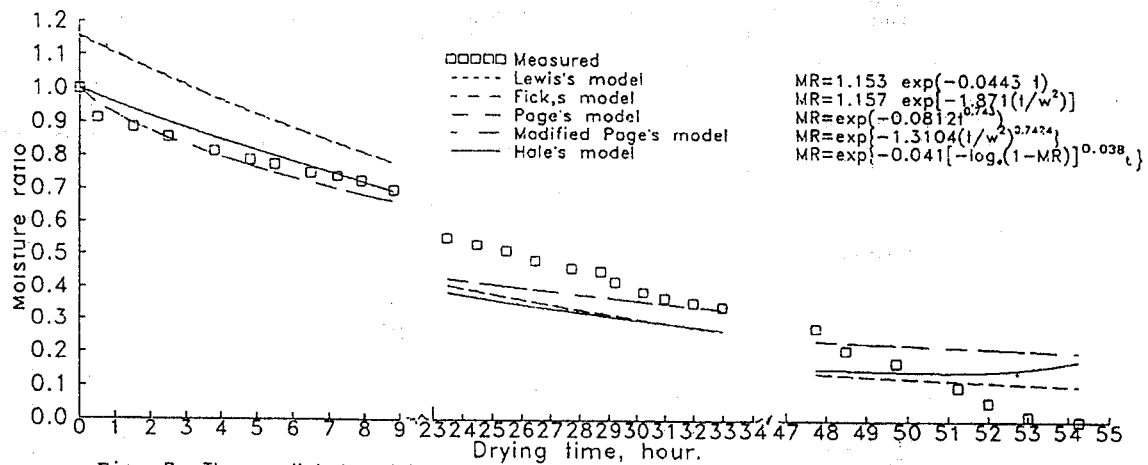


Fig. 7: The predicted moisture ratios during solar drying of grapes for tray level number 2.

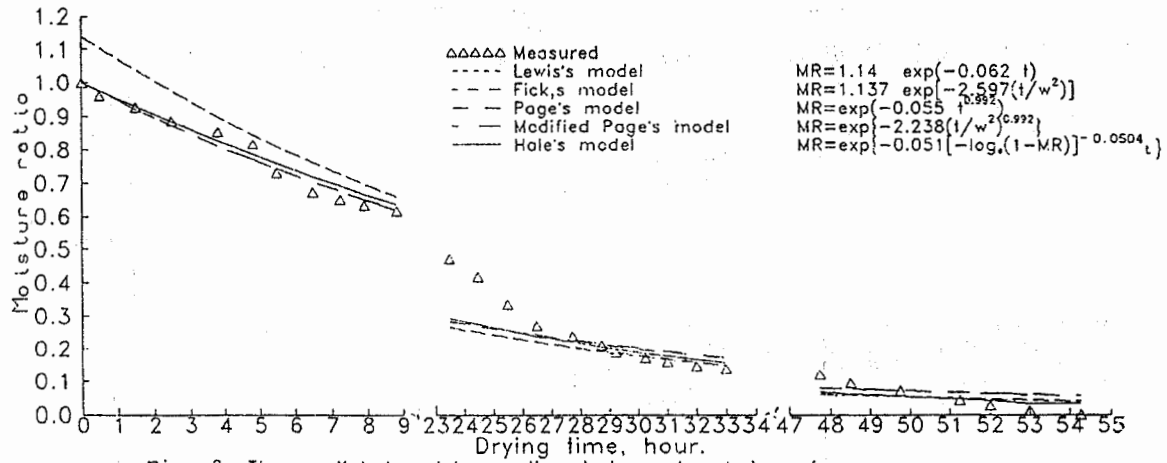


Fig. 8: The predicted moisture ratios during solar drying of grapes for tray level number 3.

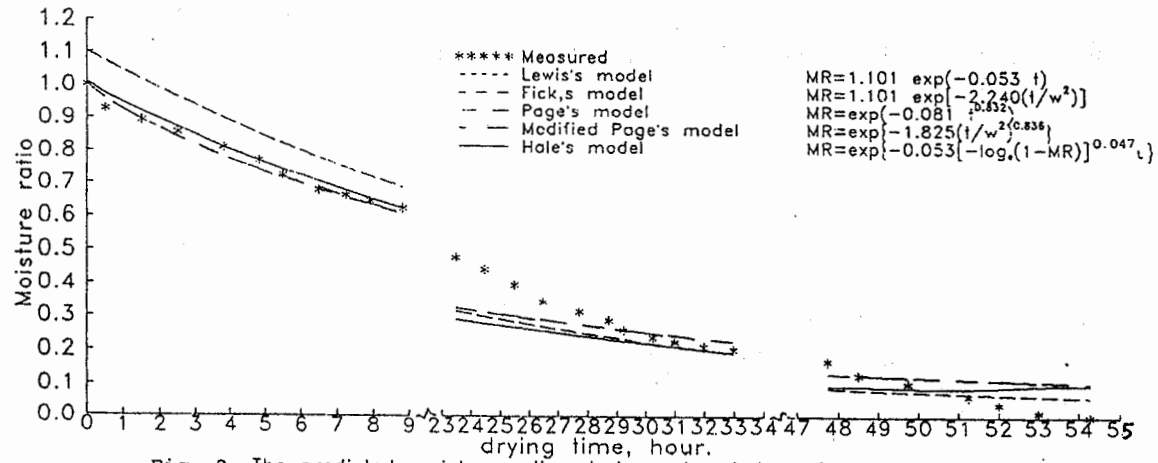


Fig. 9: The predicted moisture ratios during solar drying of grapes.

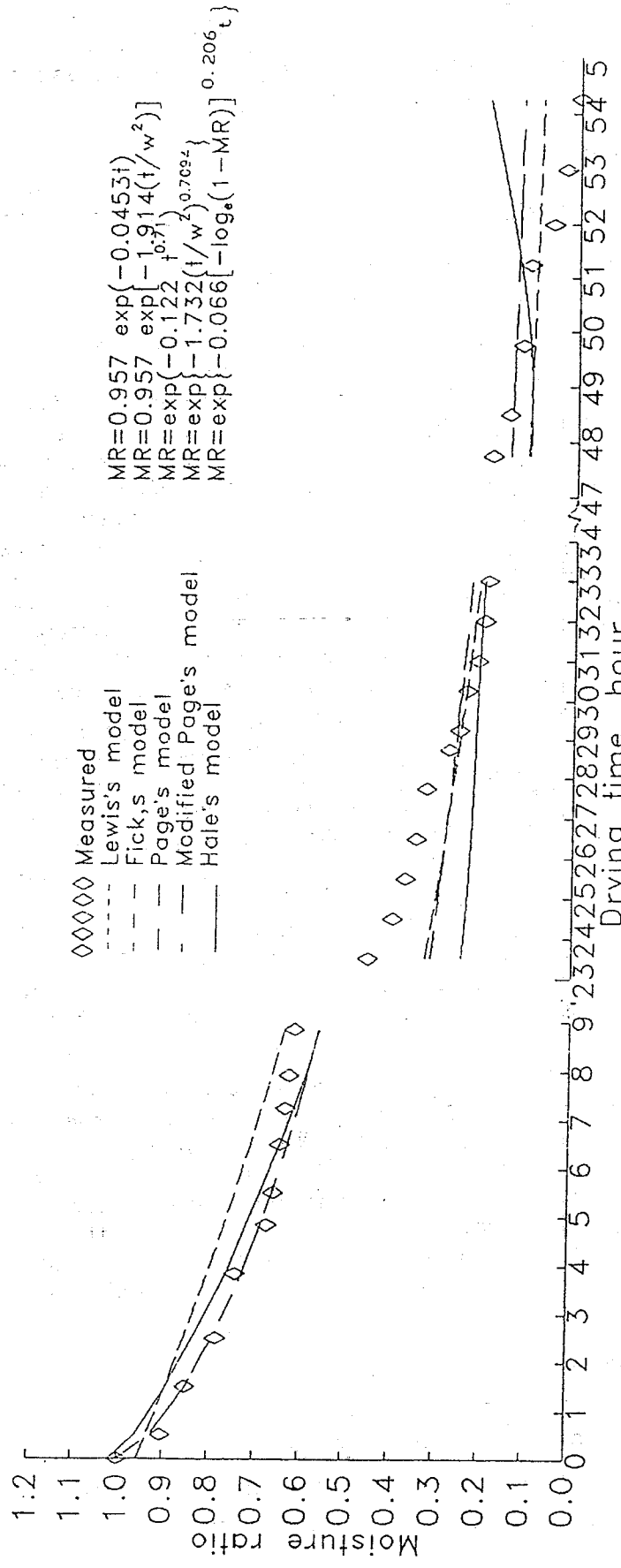


Fig. 10: The predicted moisture ratios during open sun-drying of grapes.

gives low determination coefficients. The indication of this behavior was clearly observed for tray level number 2 fitted to all models where the drying air temperature decreases from 40 to 31 °C at the last 3.0 hours on the third day.

4. CONCLUSIONS:

In the present paper, a new design and performance characteristics of multi-rack natural convection solar dryer has been described for drying various types of crops. The following conclusions are obtained:

1. The drying air temperature is significantly affected by the loaded tray level and the space between levels. It depends on the evaporated moisture from the product and the absorbed energy through the drying chamber cover. The first factor has a strong effect during the periods of rapid removal of product surface moisture, while the second has a strong effect during the periods when the moisture evaporation migrates from inside the product to the surface layer. This causes a decrease of the drying air temperatures after the first, the second and the third tray levels compared with that at the entrance during the first drying stages and the increase in the air temperature during the following stages. The percentage reduction and improvement in drying chamber temperatures and the corresponding drying time are reported.
2. The drying process of grapes is strongly dependent on the tray level and the mode of drying. The drying of grapes loaded in the first tray level nearer to the collector has the highest drying rate compared with the solar and sun-drying modes. The second tray level, loaded in the middle part of the drying chamber, has the worst drying rate, whereas the tray level located at the topmost part of the chamber gives a moderate drying rate. The solar drying rate is always higher than that for open sun-drying mode except for the time from 2.5 to 5.5 hours on the first day of drying.
3. The accuracy of the moisture ratio calculated values depends strongly on the model used in calculations, the tray level and the mode of drying. The modified Page equation is better than the exponential equation for estimating the drying rate of grapes using both solar and open sun-drying modes. The Hale's equation could satisfactorily describe the solar drying curves of grapes up to moisture contents of 36 % and 73.5 % for tray levels number 1 and 3, respectively.

NOMENCLATURE:

- a empirical constant in equations (4 and 5).
- A heat and mass transfer area, m^2 .
- b empirical constant in equations (4) and (8).
- c empirical constant in equation (5).

dM/dt	drying rate, Kg/m^2 hr.
I_t	percentage increase in air temperature.
k	empirical constant in equation (7).
m	empirical constant in equation (8).
M	moisture content, percent.
M_c	moisture content at constant rate period, percent.
M_{cr}	critical moisture content, percent.
M_f	moisture content at falling rate period, percent.
M_o	initial moisture content, percent.
MR	moisture ratio, dimensionless.
M_w	moisture content at warming-up period, percent.
n	empirical constant in equation (6) and (7).
R_t	percentage reduction in air temperature.
T_1, T_2, T_3	temperatures of air leaving tray levels numbers 1, 2, and 3, respectively; $^{\circ}C$.
T_{ci}	collector inlet temperature, $^{\circ}C$.
T_{co}	collector exit temperature, $^{\circ}C$.
w	grapes thickness, mm.
W_d	weight of the dry material at the end of the test, Kg.
W_o	initial weight, Kg.
W_t	weight of the humid material at time (t), Kg.
z	empirical constant in equation (6).

REFERENCES:

1. Kreider, J. F. and Kreith F.; Solar Energy Handbook, McGraw-Hill Book Company, New York, 18, PP. 1-28, 1981.
2. Muhibauer, W.; Present Status of Solar Crop Drying. Energy in Agriculture, 5, 121, 1986.
3. Ghosh, B. N.; Solar Energy Application in Guyana, Solar Energy Conversion 2, Selected Lectures from the 1980 International Symposium on Solar Energy Utilization, London, Ontario, Canada, August 10-24, 1980, Pergamon Press Ltd, 1981, PP. 598-612.
4. Ong, K. S.; Crop and Timber Drying in Malaysia, Proposed Plants for Studies, PP. 1654-1665.
5. Gordon, Y., Solar Crop Drying, Solar Energy Conversion 2, Selected Lectures from the 1980 International Symposium on Solar Energy Utilization, London, Ontario, Canada, August 10-24, 1980, Pergamon Press Ltd, 1981, PP. 377-396.
6. Lura, A. E.; Solar Energy in Developing Countries, Pergamon Press, Oxford, Vol.1, P. 43, 1979.

7. Sandhu, B.S., Mannan, K .D., Dhillon, G. S., Cheema, L. S.; Design Development and Performance of Multi-Rack Natural Convection Dryer; Sun 2, Proceedings of the International Solar Energy Society, Pergamon Press, New York, PP. 25-28, 1979.
8. Zaman, M. A. and Bala, B. K.; Thin Layer Solar Drying of Rough Rice, Solar Energy, Vol. 42. No. 2, PP. 167-171, 1989.
9. Diamante, L. M. and Munro, P. A.; Mathematical Modeling of the Thin Layer Solar Drying of Sweet Potato Slices, Solar Energy, Vol. 51, No. 4, PP. 271-276, 1993.
10. Mallan, K. V., Balasubramanian, T. V., and Bharadwaj, R. K.; Review on Application of Solar Energy for Drying Food Stuffs, PP. 1600-1609. Cairo.
11. Wilson, B. W.; The Role of Solar Energy in the Drying of Vine Fruit, Aust, 3, Agric. Res. Vol. 13, 662, 1962.
12. Szulmayer, W.; Thermodynamic of Sun-Drying, Paper No., Vol. 24, ISEC Conference, Paris, 1973.
13. Headley, C. and Springer, B.; A Natural Convection Solar Crop Drier, ISES Conference in Paris, 1973, IN: Solar Energy in Developing Countries, Pergamon Press, Oxford, Vol.1, P. 181, 1979.
14. Exell, R. H. B.; Basic Design Theory for Simple Solar Rice Dryer, Renewable Energy Review, J. No.1, Vol. 1, 1980.
15. Parry, J. L.; Mathematical Modeling and Computer Simulation of Heat and Mass transfer in Agricultural Grain Drying: A Review, J. Agric. Engng. Res., Vol. 32, PP. 1-29, 1985.
16. Steinfeld, A. and Segal, I.; A Simulation Model for Solar Thin Layer Drying Process, Drying Technology, 4, P. 535, 1986.
17. Akyurt, M. and Selcuk, M. K.; A Solar Drier Supplemented with Auxiliary Heating Systems for Continuous Operation, Solar Energy Vol. 14, P. 313, 1973.
18. Bolin, H. R., Stafford, A. E. and Huxsoll, C. C. , Solar Through Dryer, Solar Energy, Vol. 22, PP. 455-457, 1979.
19. Alkathiri, M. A. and Gentechev, L. N. Solar Drying of Appricot, Renewable Energy: Research and Applications, Proceeding of 1992 International Renewable Energy Conference, June 22-26, 1992, Jordan, Vol. 1, PP. 323-334, 1992.
20. Hale, O. D.; A Laboratory Technique for Evaluating and Comparing Forage Conditioning Mechanisms, J. Agric. Engng. Res., Vol. 33, PP. 243-256, 1986.
21. Diamante, L. M. and Munro, P. A.; Mathematical Modelling of Hot Air Drying of Sweet Potato Slices, Int. J. of Food Science and Tech., 26, 99, 1991.

تصميم وتطوير ودراسة اداء مجفف شمسي متعدد الرفوف

يعمل بالحمل الحر

للملخص :

يقدم البحث الحالى تركيب واختبار وكذلك دراسة خصائص الاداء لتصميم جديد لمجفف شمسي متعدد الرفوف يعمل بالحمل الحر ويستخدم لتجفيف الأنواع المختلفة للمنتجات الزراعية - يتكون التصميم الجديد من مجمع شمسي ذو شكل هرمي ناقص متصل مباشرة مع غرفة التجفيف المركبة في وضع رأسى أعلى المجمع حيث يتم فيها توزيع الرفوف واحدا تلو الآخر على أبعاد مختلفة في المجمع. استخدم عدد ٤٢ شريحة من الصاج المجلفن ذات عرض ٥ سم ومدهونة باللون الأسود ومركبة في قاعدة المجمع لامتصاص الطاقة الشمسية الساقطة وموزعة توزيعا منتظما على مسافات متساوية مقدارها ٥٢سم ومائلة بزاوية ٣٠° على الأفقى. استخدم غطاء من البلاستيك الشفاف لكل من المجمع وغرفة التجفيف - يسمح هذا التصميم من جهة بزيادة مساحة سطح المجمع وبالتالي زيادة كمية الطاقة الاشعاعية الممتصة ومن جهة اخرى بتوجيه الهواء الى مسار اطول داخل المجمع الشمسي حيث يقوم المجمع بعملية تسخين الهواء الداخل اليه والذي يمر عن طريق الحمل الحر الى غرفة التجفيف فيقوم بازالة الرطوبة من المنتج حيث يخرج مشبعا بارطوبة من قمة البرج.

استعمل أسلوبين للتجفيف: ١- أسلوب التجفيف باستعمال دوران الهواء بالحمل الطبيعي داخل المجفف - ٢- أسلوب التجفيف المفتوح باستعمال الهواء الجوى المباشر. يأخذ الأسلوب الأول في الاعتبار معالجة كل مستوى على حده داخل البرج وكذلك معالجة المجفف كوحدة واحدة- أما الأسلوب الثانى فيعتمد التجفيف على تعرض العينة للاشعاع الشمسي المباشر.

اجريت التجارب على عينات من العنب حيث تم تعيين توزيع درجات الحرارة للمجمع وعلى مستويات مختلفة للبرج. كما تم تعيين مراحل معدل التجفيف المختلفة لكل مستوى على حده وكذلك تم مقارنتها بكل من الاداء للبرج كوحدة وكذلك حالة التجفيف المباشر. ايضا يقوم البحث بالمعادلات الرياضية التى تصف عملية التجفيف لكل مستوى على حده وكذلك لكل من المجفف الشمسي والنظام المفتوح.

أوضحت الدراسة ان معدلات التجفيف للمنتج كانت اسرع وأعلى للمستويات الأقرب من المجمع بالمقارنة بالمستويات العليا وكذلك بالنسبة للتجفيفباشعة الشمس المباشر- بينما كانت العينات التى فى المستويات الوسطى فى غرفة التجفيف ذات خصائص تجفيف فقيرة. وأعطت العينات الموضوعة فى أعلى قمة البرج معدلات تجفيف معتدلة.